CALTECH ASCI TECHNICAL REPORT 120
cit-asci-tr120

Kinks in a/2<111> Screw Dislocation in Ta
Guofeng Wang, Alejandro Strachan, Tahir Cagin and William A. Goddard III

Report Documentation Page		*Form Approved* *OMB No. 0704-0188*

1. REPORT DATE **2001**	2. REPORT TYPE	3. DATES COVERED **00-00-2001 to 00-00-2001**

4. TITLE AND SUBTITLE **Kinks in a/2<111> Screw Dislocation in Ta**	5a. CONTRACT NUMBER
	5b. GRANT NUMBER
	5c. PROGRAM ELEMENT NUMBER
6. AUTHOR(S)	5d. PROJECT NUMBER
	5e. TASK NUMBER
	5f. WORK UNIT NUMBER
7. PERFORMING ORGANIZATION NAME(S) AND ADDRESS(ES) **California Institute of Technology (CalTech),Materials and Process Simulation Center,Beckman Institute (139-74),Pasadena,CA,91125**	8. PERFORMING ORGANIZATION REPORT NUMBER
9. SPONSORING/MONITORING AGENCY NAME(S) AND ADDRESS(ES)	10. SPONSOR/MONITOR'S ACRONYM(S)
	11. SPONSOR/MONITOR'S REPORT NUMBER(S)

12. DISTRIBUTION/AVAILABILITY STATEMENT
Approved for public release; distribution unlimited

13. SUPPLEMENTARY NOTES

14. ABSTRACT
We study the structure and formation energy of kinks in 1/2a<111> screw dislocations in metallic Tantalum using molecular dynamics with a first principles based many-body interatomic potential. In our study, four a/3<112> kinks are in a quadrupole arrangement in the simulation cell. We impose periodic boundary conditions in the directions perpendicular to [111] and fixed boundaries in the [111] direction. We find that two energetically equivalent, core configurations for the 1/2a<111> dislocation lead to 8 distinguishable single kinks and 16 kink pairs. The different mismatches of the core configurations along <111> direction attribute to the variations in the formation energy for different type of kinks. Formation energies for all possible kinds of isolated single kinks and kink pairs have been determined. It was found that 0.730 eV was the lowest energy cost to form a kink pair in the a/2<111> screw dislocation in Ta.

15. SUBJECT TERMS

16. SECURITY CLASSIFICATION OF:			17. LIMITATION OF ABSTRACT	18. NUMBER OF PAGES	19a. NAME OF RESPONSIBLE PERSON
a. REPORT **unclassified**	b. ABSTRACT **unclassified**	c. THIS PAGE **unclassified**	**Same as Report (SAR)**	**18**	

Standard Form 298 (Rev. 8-98)
Prescribed by ANSI Std Z39-18

Kinks in a/2<111> Screw Dislocation in Ta

Guofeng Wang, Alejandro Strachan, Tahir Cagin and William A. Goddard III

Materials and Process Simulation Center, Beckman Institute (139-74)
California Institute of Technology, Pasadena, 91125, California

Abstract

We study the structure and formation energy of kinks in 1/2a<111> screw dislocations in metallic Tantalum using molecular dynamics with a first principles based many-body interatomic potential. In our study, four a/3<112> kinks are in a quadrupole arrangement in the simulation cell. We impose periodic boundary conditions in the directions perpendicular to [111] and fixed boundaries in the [111] direction. We find that two, energetically equivalent, core configurations for the 1/2a<111> dislocation lead to 8 distinguishable single kinks and 16 kink pairs. The different mismatches of the core configurations along <111> direction attribute to the variations in the formation energy for different type of kinks. Formation energies for all possible kinds of isolated single kinks and kink pairs have been determined. It was found that 0.730 eV was the lowest energy cost to form a kink pair in the a/2<111> screw dislocation in Ta.

Key Words: Embedded-Atom-Model Potential, Dislocations, kinks, plasticity, Molecular Dynamics.

1. Introduction

The behavior of a/2<111> screw dislocations in bcc metals has been studied extensively because their mobility is the controlling factor to the plasticity of bcc metals at low temperature [1,2,3,4,5]. We have previously investigated the core structure, core energy and Peierls energy barrier and stress for a/2<111> screw dislocation in tantalum

using molecular dynamics (MD) [6]. We found that the Peierls stress is of the order of $10^{-2}\mu$ (μ is the bulk shear modulus) at zero temperature. Such high Peierls stress accounts for the low mobility of straight screw dislocations at low temperatures.

At finite temperatures, the flow stress of bcc crystals decreases sharply with increasing of the temperature, which is considered as a cause of the ductile-to-brittle transition in these metals[7]. The process of the kink pair nucleation and motion was proposed to explain how dislocations overcome an intrinsically high Peierls potential barrier. The kink pair mechanism for dislocation motion consists of the repeating processes of kink pair formation and the subsequent migration of the two kinks away from each other. Thus, the kink formation energy rather than the Peierls energy governs the mobility of the screw dislocation in bcc metals at finite temperatures. The accurate determination of kink formation enthalpies or energies is an important problem both in the experimental and theoretical communities.

For Tantalum, some experimental data on the kink pair formation enthalpy in 1/2a<111> screw dislocation has been reported. The kink pair formation enthalpy was determined to be 0.92 eV by G. Funk [8] (using γ relaxation technique), 1.24 eV by U. Rodrian and H. Schultz [9] (γ relaxation technique), 0.98 eV by M. Werner [10] (flow stress dependence on temperature and strain rate) and 0.97 eV by H. Mizubayashi et al. [11] (anelastic creep measurement). In two seminal theoretical papers [12, 13], M. Duesbury studied the structure and Peierls stress of the isolated kinks and double kink formation energy in bcc metal potassium and iron employing the atomistic simulations. Duesbury pointed out that the existence of two energetically degenerate core configurations of the a/2<111> screw dislocation leads to six different a/3<112> single kinks.

In this paper, we calculate the formation energy of single kinks and flips (also called anti-phase defect) for the a/2<111> screw dislocation using a First Principles based Embedded-Atom-Model potential [14] for Ta (named qEAM). A complete spectrum of the kink-pair formation energy, which is the summation of the corresponding single kinks and flips, is reported.

The paper is organized in the following way. In Section 2, the simulation model is described in detail. The results and findings are presented in Section 3. Equilibrium dislocation core structures, multiplicity of dislocation defects and formation energies of flips, kinks and kink pairs are discussed in Sub-section 3.1, 3.2 and 3.3, respectively. Conclusions are drawn in Section 4.

2. Model of Simulation

In order to simulate kinks and anti-phase defects in b=1/2a<111> screw dislocations we use orthorhombic simulation cells oriented along three orthogonal crystal directions that are **X**: [11-2], **Y**: [1-10] and **Z**: [111]. Our model crystal consists of three distinct construction regions along the direction of the dislocation line (**Z**). The upper and lower construction regions contain four a/2<111> screw dislocations arranged as a quadrupole; in these regions, different equilibrated dislocations are positioned and oriented in order to provide the appropriate boundary conditions to generate various types of flips and kinks. The central region contains the defect (kink or flip). In order to avoid large initial misfit on the interface between the different regions in our simulation cell, the central region is

constructed based on the elastic theory smoothing the change of core configurations along the kink and is inserted between the upper and lower construction regions.

We find that the equilibrium dislocation cores spread out in three <112> directions on {110} planes. Since there are six equivalent <112> directions normal to the dislocation line, two kinds of energy degenerate dislocation cores exist. The flip is defined as a defect where a core configuration along the screw dislocation line [15]; in this way the screw dislocation has the same X and Y positions but different relaxed core orientations on either side of the defect. The shortest (and lowest energy) kink involves the displacement of the position of the dislocation line in the (111) plane from one equilibrium position to a nearest neighbor equilibrium position; the displacement involved is 1/3 a<112>. Furthermore the screw dislocation might have the same or opposite core orientations in upper and lower regions.

We impose periodic boundary conditions in the directions perpendicular to the dislocation line. In all the simulations presented in this paper we use four dislocations in a quadrupolar arrangement; we thus have a pair of dislocations with Burgers vector b=a/2<111> and two dislocations with Burgers vector b=a/2<-1-1-1>. Such arrangement minimizes the misfit of atoms on the periodic boundary due to the effects of periodic imagesand leads to zero total force on straight dislocations. Finally, we use free boundary conditions in the <111> direction; we define two 5 b thick regions where atom positions are fixed to the relaxed dislocation configuration during the simulation in both ends of simulation cell. Atoms in the region between two fixed boundaries are allowed to move to minimize total potential energy. The relaxed region needs to be long enough to minimize the effect of the fixed boundaries on the flip and kink formation energy. We

find that the formation energy of the kink typically changes only 0.2% when the cell length along z is increased from 90 b to 150 b. In this study, we employed the simulation cell whose geometry was 5a[1-12], 9a[1-10] and 150a/2[111]. Our cell contains 40500 atoms (37800 movable) in a simulation cell of volume 40.7 x 42.3 x 431.8 $\mathring{A}^3$.

3. Results and Discussion

3.1 Equilibrated dislocation core structure

In our study, the initial screw dislocation quadrupoles were constructed based on the displacements obtained from elasticity theory and the total strain energy of the system was minimized to obtain the equilibrium core configurations. Using the qEAM force field we find that the equilibrium dislocation core has three fold symmetry and spreads out in three <112> directions on {110} planes. There are 6 equivalent <112> directions on the (111) plane which lead to two kinds of core configurations both for dislocation with the Burgers vector a/2[111] and for dislocation with the Burgers vector -a/2[111]. Figure 1 shows the differential displacement (DD) maps of the different core configurations. Figures 1(a) and (b) show two cores for a dislocation with b=1/2a<111> and Figures 1(c) and (d) show the cores with b=1/2a<-1-1-1>. In DD maps atoms are represented by the circles and projected on a (111) plane of the bcc lattice; the arrows represent the relative displacements, due to the dislocations, in the [111] direction between neighboring atoms with respect to their positions in the perfect bcc crystal. The direction of the arrows represents the sign of the displacements and the magnitude of the arrow is proportional to the relative displacement between the corresponding atoms.

When an arrow touches the two atoms, the relative displacement between these two atoms is 1/3 b. As already mentioned the two cores are energetically degenerate in the sense both of the core energy and elastic interaction energy. In Figure 2 we show the atomic displacements in the [111] direction of the relaxed dislocations referenced to the displacements obtained using elasticity theory. The panels (a)-(d) correspond to the same cores as those in Figure 1. The displacement differences for atoms except the 6 columns closest to the dislocation line are less than +/- 0.05 Å. Such result demonstrates that the elastic theory describes the elastic field of the dislocation pretty well and the elastic theory fails at the core region of the dislocation as expected. A most important feature seen in Figure 2 is that three central atoms of the dislocation translate simultaneously 0.267Å (~0.09b) either in [111] direction or [-1-1-1] direction after the relaxation. This phenomenon is called polarization of the dislocation core [17]. The dislocation is named P (positive) if the three central atoms translate along [111] while the dislocation is called N (negative) if the three central atoms shift along [-1-1-1]. It should also be noticed that the dislocations have the same polarization regardless the orientation the Burgers vector b if their cores spread out along the same <112> directions. Such observation is essential for us to guarantee that the four dislocations in our cell have the same type of flip or kink defect.

3.2 Multiplicity of dislocation defects

The existence of N-type and P-type dislocations [shown schematically in Figure 3(a)] leads to multiple possible configurations of the flips and kinks. Figure 3(b) shows a

diagram of two types of flips as a result of the core polarization. The three columns of atoms closest to the dislocation line are under compression in a P-N flip and in a tensile state in an N-P flip. Such that the P-N flip and the N-P flip are two distinct configurations for dislocation flips. As mentioned, we focused on the kinks where the two dislocation segments are in nearest neighboring equilibrium positions (separated by a/3<112>). We define the kink vector as the vector that goes from the equilibrium dislocation position below the kink to the equilibrium dislocation position above the kink. There are six possible <112> directions but only two need to be considered by symmetry, this leads to two kink directions which we will call left (L with kink vector -a/3[11-2]) and right (R with kink vector a/3[11-2]). For each kink vector, there are four combinations of core configurations leading to 8 possible kinks: NRP, NRN, PRP, PRN, NLP, NLN, PLP and PLN. All possible distinct a/3<112> single kinks are shown in the Figure 3(c). Among these kinks, the NRN and PRP are energy degenerate and related by symmetry operations, so are the NLN and PLP kinks.

3.3 Formation energy of flips, kinks and kink pairs

The dislocation core configurations, their polarization and the multiplicity of flips and kinks have been discussed in the previous sections. With such knowledge, it is practical to construct a dislocation quadruple such that all dislocations have the same type of flips or kinks. The total strain energy of the equilibrated dislocation quadrupole with defects can be expressed as the summation of the defect (flip or kink) formation energies, the

defect elastic interaction energy and energy of the quadrupole with dislocations without defects.

The elastic interaction between flips is zero since the dislocation line remains unchanged and so does its elastic field. Thus, the flip formation energy is simply the total energy of the quadrupolar arrangement of dislocations with flips minus that of the perfect dislocations divided by the number of kinks. Figure 3 (b) shows the results obtained with the qEAM FF.

The interaction energy between kinks is not zero. Nevertheless, as a first order approximation, we neglect their interaction and calculate the kink formation energy as explained for the flips. The resulting formation energies are shown in Figure 3 (c). The systematical error introduced by neglecting the elastic interactions for a periodic kink quadrupole can be estimated using the isotropic elastic theory and assuming that the kinks are pure <112> edge segments perpendicular to the dislocation lines. [16] For our simulation cell, we estimate the interaction energy to be -0.027 eV, i.e. the kink formation energies shown in Figure 3 (c) should be increased by 0.027eV. It is worth mentioning here that the equilibrated kink is not an edge line segment perpendicular to the dislocation line. Actually, the kink has very large screw component; we find that the kink length in the [111] direction is ~10b (~28.8 Å), an order of magnitude larger than its extent in the [112] direction (~2.71 Å). . Thus, the expected systematical error in computing the kink formation energy in our study is much smaller the our estimation of 0.027 eV. In Figure 3, flips and kinks are drawn schematically to show the core configuration misfit.

In addition to the single kink at which the dislocation line lies across a Peierls energy hill, there are kink pairs constituted by a left kink and a right kink. These kink pairs can be formed by thermal fluctuation and their nucleation and motion are thought to be important in low temperature deformation processes [16]. If the separation between the left and right kink is large enough, the formation energy of a kink pair is just the sum of formation energy of two component kinks. Since there are both 4 kinds of left kinks and 4 kinds of right kinks, there are 16 ways to combine them to form a kink pair. In some cases, one or two flips are required to fulfill the requirement of core configuration. The configurations and formation energies for all kink pairs have been listed in the Table I. We find that the NRP-PLN kink pair has the lowest formation energy which is 0.73 eV.

4. Concluding remarks

In a summary, we found that there were two types of equilibrated core configurations for a/2<111> screw dislocation. These two energy degenerate core configurations have polarizations with the opposite sign, namely three columns of atoms closest to these two types of dislocations translate simultaneously in the opposite <111> directions as compared to the elasticity theory displacements. Two types of core configurations lead to 2 kinds of dislocation flips and 8 kinds of dislocation single kinks. We calculated the formation energies for these dislocation defects by minimizing the energy of a dislocation quadrupole containing the defects to an equilibrated state. Kink pairs are the combination of a pair of left and right single kinks and one or two flips that adjust the core configurations. We have computed formation energies for all 16 kinds of kink pairs and

found that the NRP-PLN kink pair has the lowest nucleation energy which is 0.73 eV. We found that the formation energies of the right kinks [NRP, NRN (PRP) and PRN] are very similar, decreasing by 0.02 eV from one to the other. On the other hand the formation energy of the left kinks [PLN, PLP (NLN) and NLP]differ by approximately by 0.50 eV. The different behavior of L and R kinks can be explained analyzing their core structures. We find that the PLP kink (0.6 eV) is formed by a PLN kink (0.11 eV) plus a NP flip (0.57 eV). The NLP kink (1.12 eV) is formed by a NP flip (0.5 eV), a PLN kink (0.11 eV) and another NP flip (0.5 eV). The presence of the high energy NP flip explains the large energy differences among the left kinks. On the other hand the right kinks differ by the low energy PN flip, leading to very similar energies. A detailed structural analysis of the different kinks will be published elsewhere. [18]

Acknowledgement

References:

1. Vitek, V., Crystal Lattice Defects, 5 (1974) 1.

2. Xu, W. and Moriarty, J.A., Phys. Rev. B, 54 (1996) 6941.

3. Xu, W. and Moriarty, J.A., Comput. Mater. Sci., 9 (1998) 348.

4. Moriarty, J.A., Xu, W., Soderlind, P., Belak, J., Yang, L.H. and Zhu, J., Eng. Mater. Technol., 121 (1999) 120.

5. Ismail-Beigi, S. and Arias, T.A., Phys. Rev. Lett., 84 (2000) 1499.

6. Wang, G., Strachan A., Cagin, T. and Goddard, W.A., Mater. Sci. and Eng. A, 309 (2001) 133..

7. Wen, M. and Ngan, A.H.W., Acta Mater., 48 (2000) 4255.

8. Funk, G., Dissertation, University Stuttgart, 1985.

9. Rodrian, U. and Schultz, H., Z. Metallk., 73 (1982) 21.

10. Werner, M., Phys. Stat. Sol. (a), 104 (1987) 63.

11. Mizubayashi, H., Egashira, H. and Okuda, S., Acta Metall. Mater., 43 (1995) 269.

12. Duesbery, M.S., Acta Metall., 31 (1983) 1747.

13. Duesbery, M.S., Acta Metall., 31 (1983) 1759.

14. Strachan A., Cagin, T., Gulseren, O., Mukherjee, S., Cohen, R.E. and Goddard W.A., Phys. Rev. B, submitted.

15. Hirth, J.P., Acta Mater., 48 (2000) 93.

16. Hirth, J.P. and Lothe, J., Theory of Dislocations, Krieger, Melbourne, FL, 1992.

17. Seeger, A. and Wuthrich, C., Nuovo Cimento, 33 (1976) 38.

18. Wang, G., Strachan A., Cagin, T. and Goddard, W.A., in preparation.

Figure Caption

Figure 1, Differential displacement map (DDM) of equilibrated dislocation core structures. Figure (a) and (b) are showing two types of core configurations of dislocation with b=a/2[111], while Figure (c) and (d) show core configurations of dislocation with b=a/2[-1-1-1]. The arrangement of figures is same as Figure 2.

Figure 2. (111) projection map of equilibrium screw dislocation cores. Atoms are represented by circles and projected on a (111) plane of bcc lattice. Arrow from each atom indicates the relaxation parallel to the dislocation line relative to displacement field predicted by isotropic elastic theory. The magnitudes of such relaxation of central six columns of atoms are printed next to corresponding atom and in the unit of Å. The arrangement of figures is same as Figure 1.

Figure 3. (a) Schematic drawings of N-type dislocation core and P-type dislocation core. Arrows indicate whether three central columns of atoms move toward or outward defect (flip or kink) region.

      (b) Sketches and formation energies of flips.

      (c) Sketches and formation energies of isolated single kinks.

Table I, Schematic drawings and Formation energies of kink-pairs. Formation energies are printed in the figure and in the unit of eV. N and p stands for N-type or P-type dislocation core, respectively. NxP and pxn represent N-P flip or P-N flip.
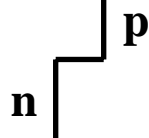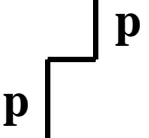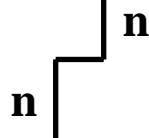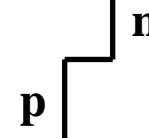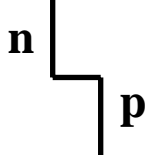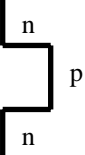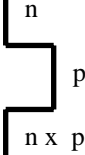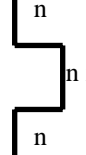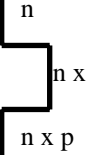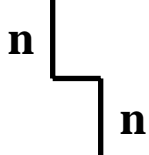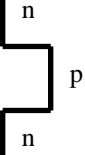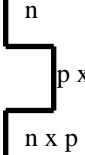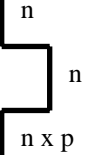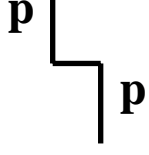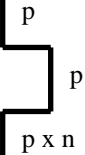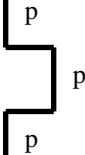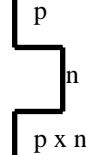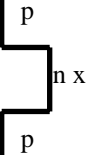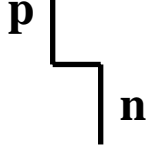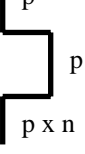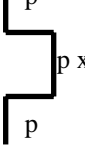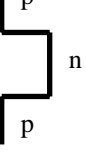
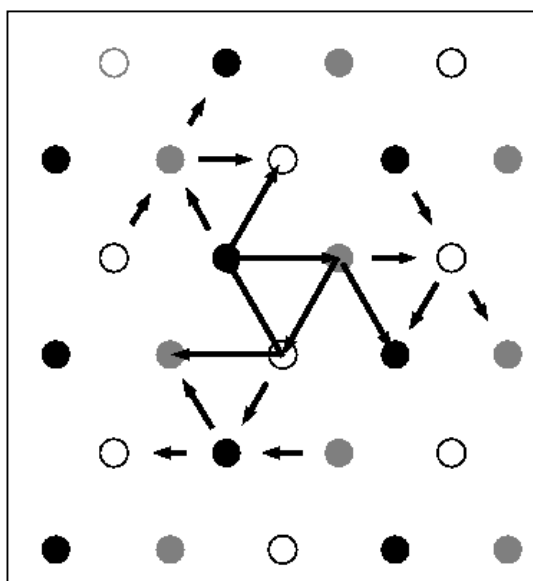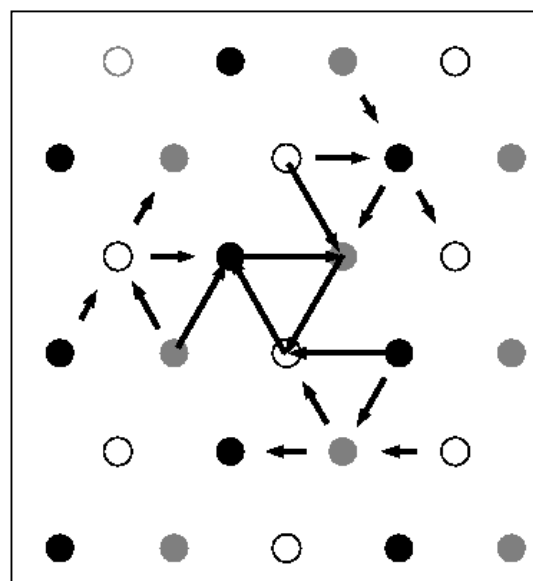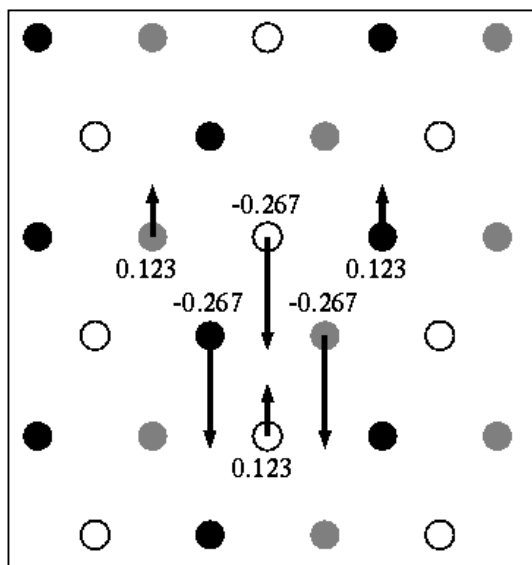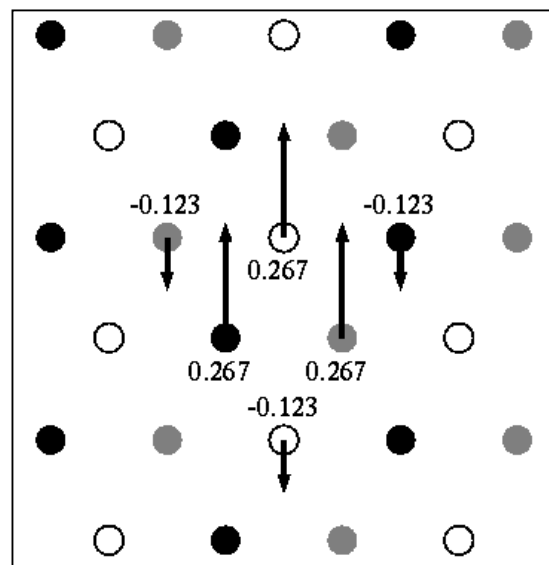|	**n / p**	**p / p**	**n / n**	**p / n**
n / p	0.730	1.280	1.280	1.830
n / n	1.225	1.775	1.200	1.750
p / p	1.225	1.200	1.775	1.750
p / n	1.750	1.725	1.725	1.700

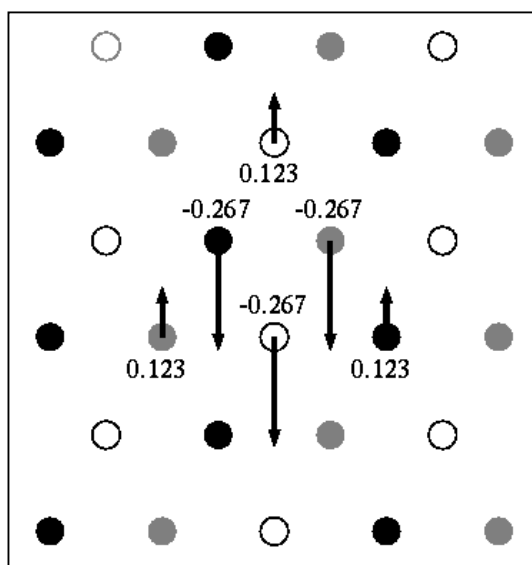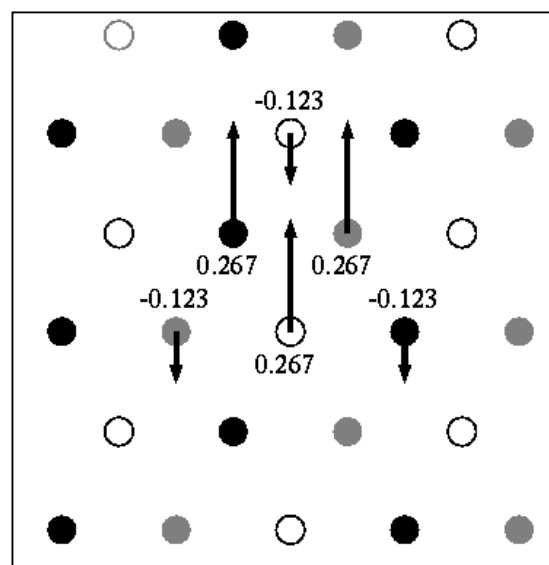Figure 1 G.Wang et al
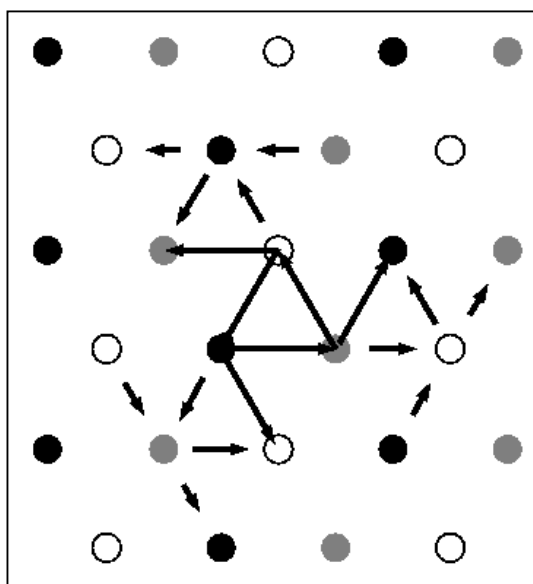
(a)
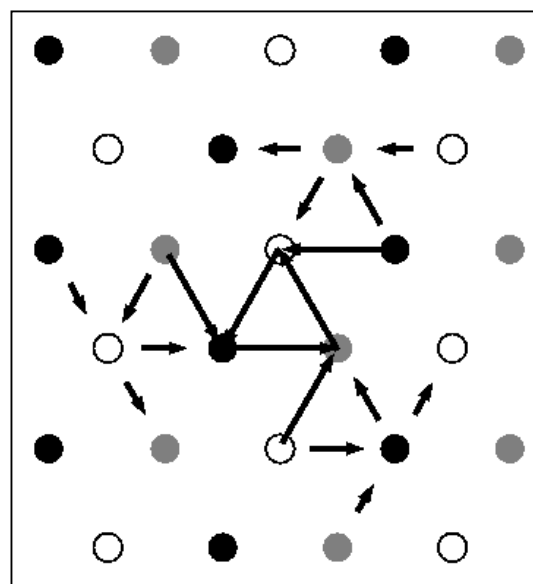
(b)

(c)

(d)

Figure 2 G. Wang et al

Figure 3 G. Wang et al

(a)

N-type dislocation   P-type dislocation

(b)   Flips (Anti-phase defects)

P-N flip   N-P flip

ΔH=0.005 eV   ΔH=0.57 eV

(c)   Single kinks

NRP kink   NRN kink   PRP kink   PRN kink

ΔH=0.62 eV   ΔH=0.60 eV   ΔH=0.60 eV   ΔH=0.58 eV

NLP kink   NLN kink   PLP kink   PLN kink

ΔH=1.12 eV   ΔH=0.60 eV   ΔH=0.60 eV   ΔH=0.11 eV